

Supporting information

Designing Surface Chemistry of Silver Nanocrystals for Radio-frequency Circuit Applications

*Hanju Oh^{#1,3}, Seung-Wook Lee^{#2}, Minsoo Kim³, Woo Seok Lee^{†2}, Mingi Seong^{†2}, Hyungmok Joh^{†2}, Mark G. Allen³, Gary S. May^{1,4}, Muhannad S. Bakir^{*1}, Soong Ju Oh^{*†2}*

1 School of Electrical and Computer Engineering, Georgia Institute of Technology, Atlanta, GA, United States

2 Department of Materials Science and Engineering[†]& Department of Semiconductor Systems Engineering[‡], Korea University¹⁴⁵, Seoul 02841, Republic of Korea

3 Singh Center for Nanotechnology & Department of Electrical and Systems Engineering, University of Pennsylvania, Philadelphia, PA, United States

4 University of California at Davis, CA, United States

Corresponding Author

* E-mail: sjoh1982@korea.ac.kr, mbakir@ece.gatech.edu

Discussion

Calculations of sizes of as-synthesized and TBAB-, H₂AuCl₄-, N₂H₄-treated Ag NCs, and Au shell thickness on H₂AuCl₄- and N₂H₄-treated Ag NC

We calculated the size of the Ag NCs after TBAB-, H₂AuCl₄-, and N₂H₄-treatment using the following Scherrer equation (equation S1):

$$\tau = \frac{K \times \lambda}{\beta \times \cos \theta} \quad \text{Eq. (S1)}$$

where τ is the mean size of the NCs, K is a dimensionless shape factor (about 1.2), λ is the X-ray wavelength of the copper $K\alpha$ (0.154 nm), β is the full width at half maximum, and θ is the Bragg angle.

By extracting β and θ from the Ag (111) plane in the XRD plot of Figure 2d, the average sizes of the NCs were calculated using equation (1), yielding 3.4 nm, 23.0 nm, 23.2 nm, and 23.1 nm for as-synthesized, TBAB-, H₂AuCl₄-, and N₂H₄-treated Ag NCs, respectively. SEM and TEM image shows that the size of the ligand exchanged Ag NCs are around 50-200 nm. The difference could be understood by the nature of polycrystalline particles. As seen in SEM or TEM, each polycrystalline particle has single crystalline grains. The average size of Ag NCs were ~100nm and the size of individual grains in NCs is ~23 nm.

To estimate the Au shell thickness, Ag-Au core-shell structure with a radius of core Ag, r , and the thickness of Au shell, x , is assumed for H₂AuCl₄- and N₂H₄-treated Ag NC. From TEM image (TBAB-treated Ag NCs), the size of core Ag NC ($2r$) is assumed as 100 nm, and thus r is 50 nm. From EDX data, volume ratios of Ag and Au in H₂AuCl₄- and N₂H₄-treated Ag NC are 86 : 14 and 88 : 12, respectively. Therefore, the thickness of Au shell, x , can be estimated by following equations:

$$r^3 : ((r + x)^3 - r^3) = \text{Ag} : \text{Au (volume ratio)}$$

The thickness of Au shell, x is calculated to 3.0 nm and 2.2 nm for H₂AuCl₄- and N₂H₄-treated Ag NC, respectively.

Oxidation resistance and stability analysis

In the case of the ligand exchanged and Au coated Ag NC thin film, the electrical resistance slightly increased with increasing time. N₂H₄-treated films exhibited only slight changes in their electrical resistance over a period of 30 days. We analyzed the oxidation resistance of the films under extreme conditions. The samples were treated with UV-ozone for 30 min, after which their resistances were measured. The resistances of ligand-exchanged, Au and reduced Ag NC thin films increased by 208%, 12%, and 12.5%, respectively.

High Frequency Electrical Characteristics Simulations

To understand the high-frequency electrical characteristics of Ag NC conductors, electromagnetic simulations were implemented using ANSYS High Frequency Structure Simulator (HFSS) v18.2, which is a commercial software based on the finite element method (FEM). The transmission line and circuit models were built in the HFSS according to the actual structures that we fabricated, as shown in Supplementary Figure 3. The transmission lines and pads are designed based on ground-signal-ground (GSG) coplanar waveguide (CPW) with 2-port lumped network. The width and gap of signal lines were set to 250 and 100 μm to achieve 50 Ω characteristic impedance at a polyethylene terephthalate (PET) substrate with thickness of 100 μm . The dielectric constant and loss tangent of PET were set to 3 and 0.002 as the PET manufacturer provided. The width of upper ground planes was optimized until it does not change the total scattering parameter values. We set the bulk conductivity of thin metal layers as a variable and varied it from 1×10^5 to 1×10^7 S/m to calculate the effective conductivity of the fabricated Ag NC films, as illustrated in Figure S3a. The results show that the electrical conductivity of the Br-treated Ag NC films is in line with that of the transmission line with a bulk conductivity of 2×10^5 S/m. The Ag NC films with 1mM Au concentration correspond to the transmission lines of bulk conductivities between 1×10^6 and 2×10^6 S/m, while the electrical conductivity of Ag NC films with 5mM Au concentration well agrees with that of transmission lines with bulk conductivity of 2×10^6 S/m. Subsequently, the passive circuits are built in HFSS based on the transmission line analysis and the electrical circuit parasitic values were extracted up to 20 GHz. Overall, the results agree well with the results of HFSS simulations with less than 10% error on average.

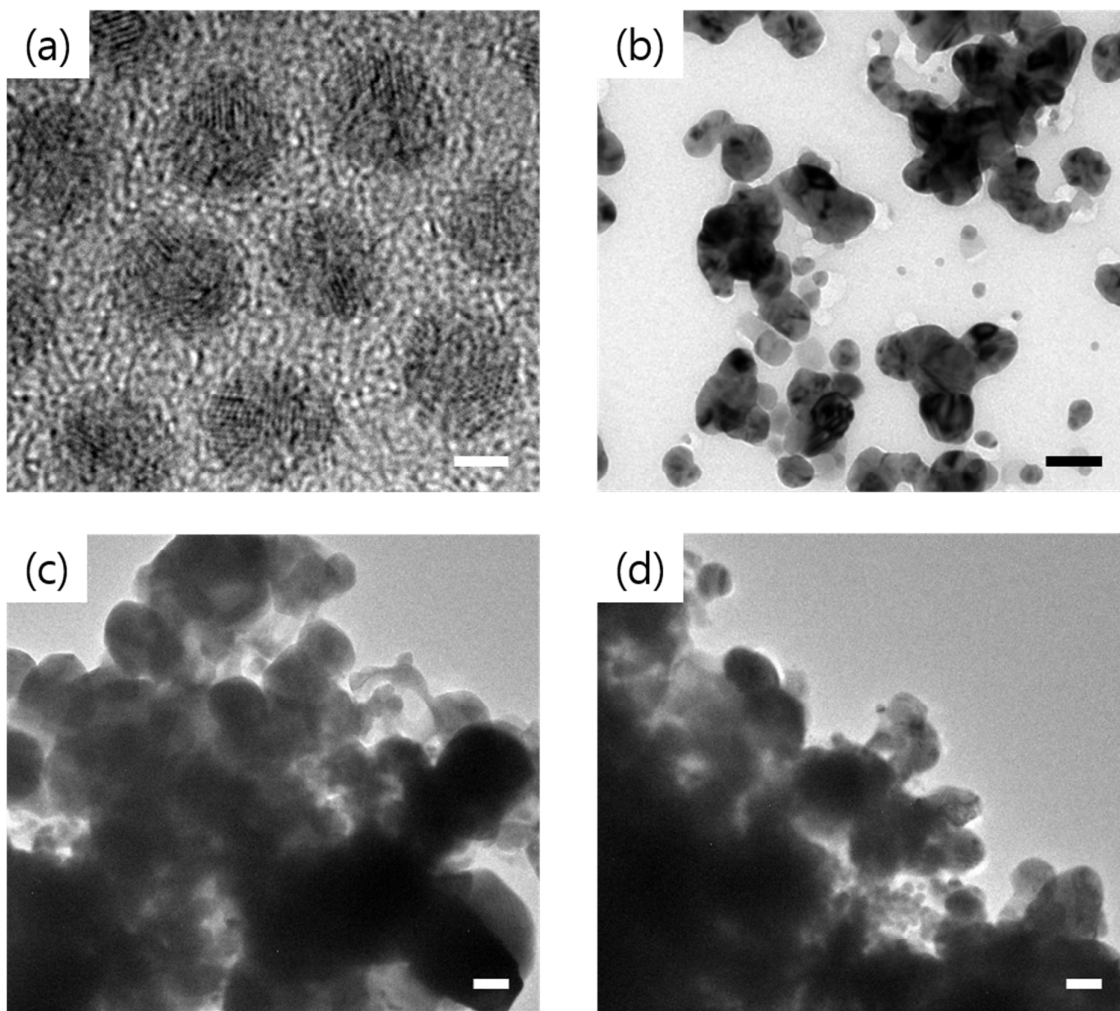


Figure S1. TEM images of (a) as-synthesized, (b) TBAB-treated, (c) Au-coated, and (d) reduced Ag NCs. The scale bar is 2 nm for a) and 50 nm for b), c) and d)

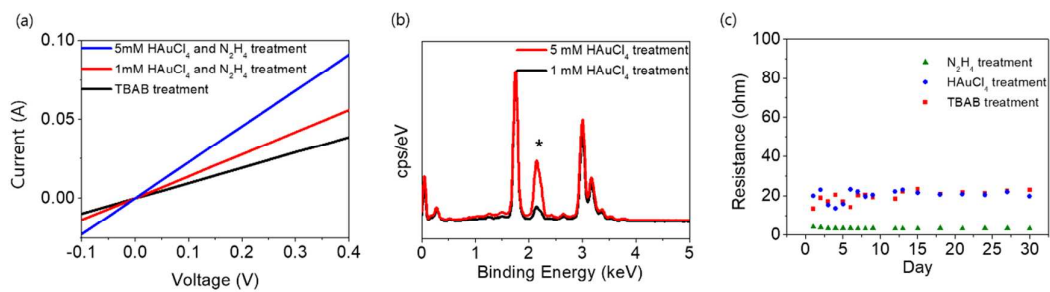


Figure S2. (a) I-V curves of the Ag NC thin films with different treatments. (b) EDX spectra of 1 mM and 5 mM AuCl_4 -treated Ag NC thin films (* indicates Au). (c) Variation in the resistance of Ag NC thin films with different treatments as a function of time.

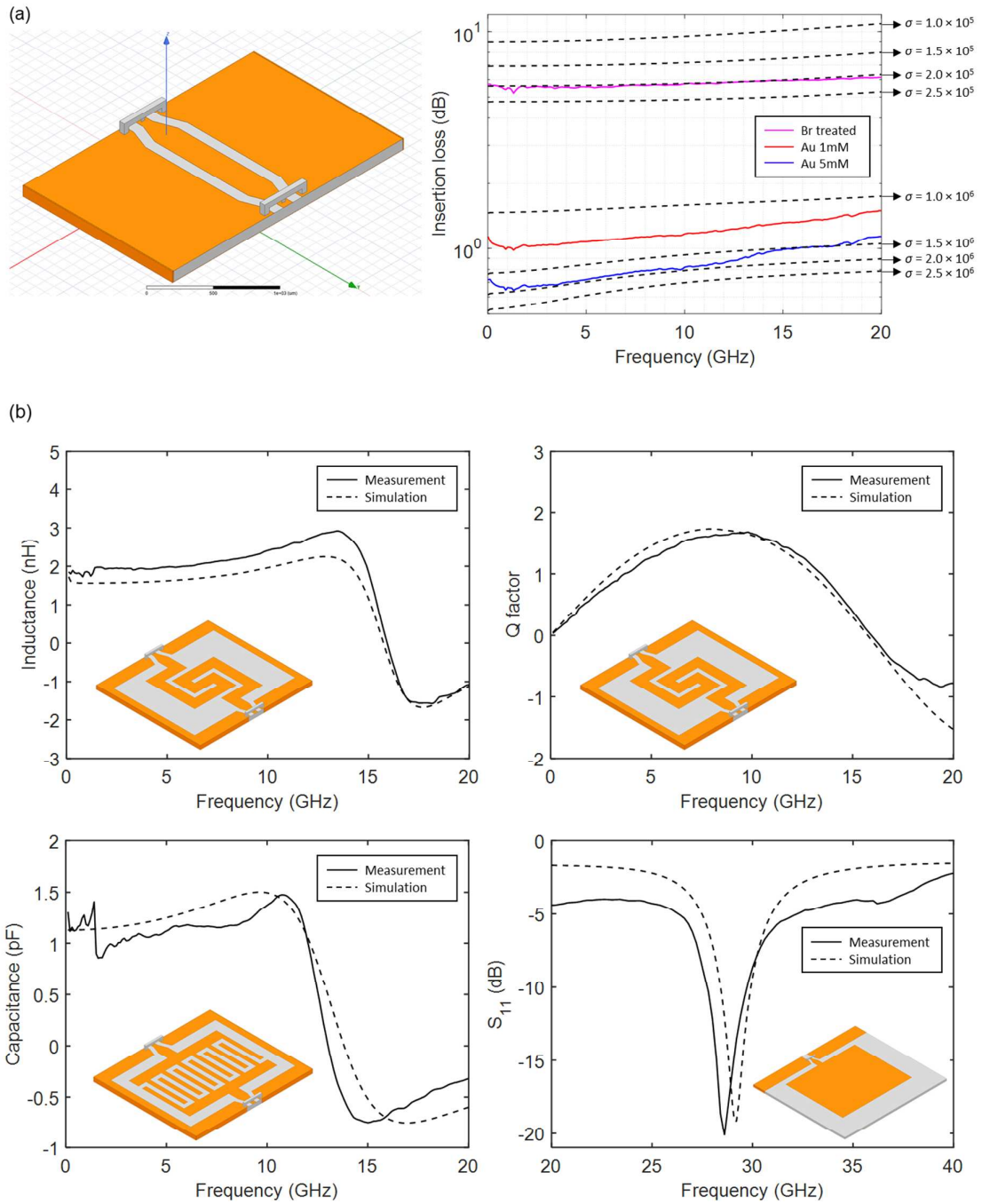


Figure S3 (a) High frequency structure simulation (HFSS) schematic and (b) result for conductor-backed coplanar waveguide transmission lines.

Table S1: Comparison of Ag NP technology in the literature

	Bulk Ag	This work	Conventional Ag NP			Ag NP with State-of-the-art Sintering Process				
Paper	N/A	This work	IEEE APS 2005 ¹	IEEE TCPMT 2017 ²	IEEE IMS 2016 ³	ACS Nano 2010 ⁴	Adv. Mat. 2012 ⁵	J. Mat. Chem. 2010 ⁶	Adv. Mat. 2006 ⁷	ACS Nano 2013 ⁸
Sintering process	N/A	Ligand exchange (TBAB)	Laser	High-T (180/150°C)	High-T (200°C)	Room T Polymer (PDAC)	Microwave & Photonic sintering*	UV-cure	Microwave radiation @2.45GHz	Focused laser scanning
Conductivity (S/m)	6×10^7	2×10^6	1.6×10^6	$5.7/6.9 \times 10^6$	$\sim 10^7$	1.4×10^6 1.4×10^7	$2.5/1.7 \times 10^7$	6.5×10^6	3×10^6	1.4×10^7
Applications	N/A	RF passive circuits	RFID tag	Substrate-integrated-waveguide	RF interconnect & antennas	Flexible and plastic electronics	Roll-to-roll applications	Technology demonstration		Flexible and transparent applications

REFERENCES

- (1) Nikitin, P. V.; Lam, S.; Rao, K. V. S. Low Cost Silver Ink RFID Tag Antennas. *IEEE APS* **2015**, *2B*, 353-356.
- (2) Kim, S.; Shamim, A.; Georgiadis, A.; Aubert, H.; Tentzeris, M. Fabrication of Fully Inkjet-Printed Vias and SIW Structures on Thick Polymer Substrates. *IEEE Trans. Comp. Pack. Manuf. Tech.* **2016**, *6*, 486-495.
- (3) Tehrani, B. K.; Cooky, B. S.; Tentzeris, M. Inkjet-Printed 3D Interconnects for Millimeter-Wave System-on-Package Solutions. *IEEE Int. Microw. Symp.* **2016**, 1-4.
- (4) Magdassi, S.; Grouchko, M.; Berezin, O.; Kamyshny, A. Triggering the Sintering of Silver Nanoparticles at Room Temperature. *ACS Nano* **2010**, *4*, 1943–1948.
- (5) Perelaer, J.; Abbel, R.; Wünsch, S.; Jani, R.; Lammeren, T. V.; Schubert, U. S. Roll-to-Roll Compatible Sintering of Inkjet Printed Features by Photonic and Microwave Exposure: From Non-Conductive Ink to 40% Bulk Silver Conductivity in Less Than 15 Seconds. *Adv. Mater.* **2012**, *24*, 2620-2625.
- (6) Valetton, J. J. P.; Hermans, K.; Bastiaansen, C. W. M.; Broer, D. J.; Perelaer, J.; Schubert, U. S.; Crawford, G. P.; Smith, P. J. Room temperature preparation of conductive silver features using spin-coating and inkjet printing. *J. Mater. Chem.* **2010**, *20*, 543–546.
- (7) Perelaer, J.; Gans, B.-J. D.; Schubert, U. S. Ink-jet Printing and Microwave Sintering of Conductive Silver Tracks. *Adv. Mater.* **2006**, *18*, 2101–2104.
- (8) Hong, S.; Yeo, J.; Kim, G.; Kim, D.; Lee, H.; Kwon, J.; Lee, H.; Lee, P.; Ko, S. H. Nonvacuum, Maskless Fabrication of a Flexible Metal Grid Transparent Conductor by Low-Temperature Selective Laser Sintering of Nanoparticle Ink. *ACS Nano* **2013**, *6*, 5024–5031.